

Multivalent Choline Dendrimers as Potent Inhibitors of Pneumococcal Cell-Wall Hydrolysis**

Víctor M. Hernández-Rocamora, Beatriz Maestro, Bas de Waal, María Morales, Pedro García, E. W. Meijer, Maarten Merkx,* and Jesús M. Sanz*

Streptococcus pneumoniae (pneumococcus) causes multiple illnesses in humans, including pneumonia, meningitis, and acute otitis media.^[1] It especially affects children under two years of age and the elderly, with an estimated 1.6 million deaths per year.^[2] The fight against this pathogen is hindered by the increase of antibiotic resistance and the limited efficacy of current vaccines.^[1] A characteristic feature of the pneumococcal cell wall is the presence of teichoic acid units decorated with phosphocholine groups^[3] (Figure 1 a). These multivalent architectures serve as attachment sites for a variety of surface-exposed choline-binding proteins (CBPs) that are involved in processes essential for virulence, such as cell-wall division, the release of bacterial toxins, and adhesion to the host.^[4] All CBPs contain a characteristic choline-binding module (CBM) consisting of several choline-binding repeats, sequences of about 20 amino acids with a loop- β -hairpin structure, that are arranged into a left-handed superhelix.^[5,6] Two consecutive repeats configure a choline-binding site by means of three aromatic residues. The best characterized member of these

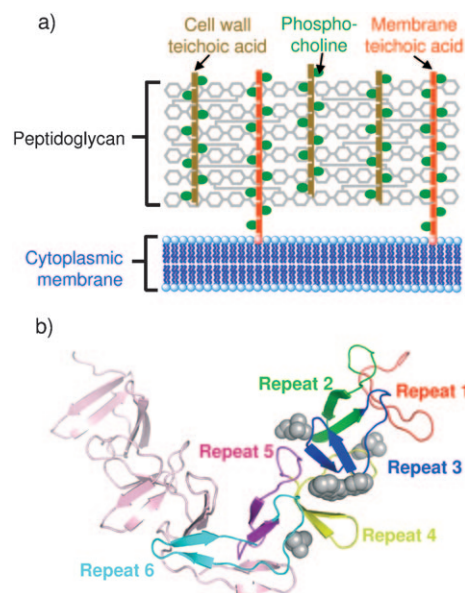


Figure 1. a) Schematic representation of the *S. pneumoniae* cell-wall structure showing the multivalent arrangement of phosphocholine groups. b) X-ray structure of the choline-binding module of the LytA amidase (C-LytA) based on PDB 1HCX.^[5] Each strand of the homodimer contains six repeats, each composed of a β hairpin and a large loop that together constitute four choline-binding sites, which are occupied in the crystal structure by three choline residues and a dodecylamine-*N,N*-dimethyl-*N*-oxide molecule (gray spheres). The image was prepared using the software package PyMol (Delano Scientific LLC).

choline-binding modules, the C-terminal moiety of the LytA amidase (C-LytA),^[7,8] contains six of these repeat sequences that together form four choline-binding sites^[5] (Figure 1 b). Because CBPs are common to all serotypes, they are attractive drug targets for the treatment of pneumococcal diseases. Exogenously added choline and choline analogues competitively inhibit the binding of CBPs to the cell wall, blocking cell separation and the characteristic autolysis of *S. pneumoniae* at the end of the stationary phase of growth, inducing instead the formation of long chains^[9] or even preventing growth.^[10] These effects are thought to reduce bacterial virulence by preventing the release of toxins upon cell autolysis and limiting the dissemination of the bacteria on the host tissue during infection.^[11] However, the required concentrations of these compounds (in the millimolar range) are much too high for their therapeutic use as antimicrobial agents *in vivo*.

The weak interaction between choline and a single choline-binding site^[10,12] explains the need for tandem chol-

[*] V. M. Hernández-Rocamora, Dr. B. Maestro, Dr. J. M. Sanz
Instituto de Biología Molecular y Celular
Universidad Miguel Hernandez
Avda. de la Universidad s/n, 03202 Elche (Spain)
Fax: (+34) 966-588-758
E-mail: jmsanz@umh.es
Homepage: <http://ibmc.umh.es/jmsanz/jmsanz.htm>

B. de Waal, Prof. E. W. Meijer, Dr. M. Merkx
Laboratory for Chemical Biology
Eindhoven University of Technology
5600MB, Eindhoven (The Netherlands)
Fax: (+31) 40-245-1036
E-mail: m.merkx@tue.nl

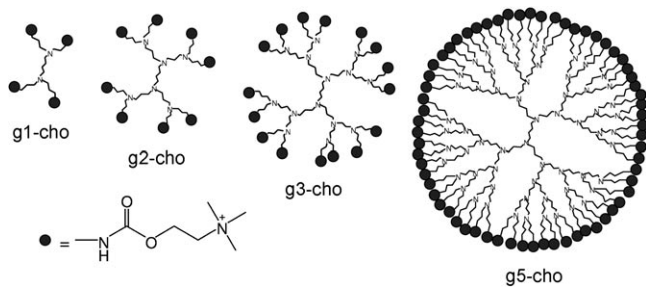
M. Morales, Dr. P. García
Departamento de Microbiología Molecular
Centro de Investigaciones Biológicas, CSIC
and
CIBER de Enfermedades Respiratorias (CibeRes)
Ramiro de Maeztu, 9, 28040 Madrid (Spain)

[**] We would like to thank Xianwen Lou for GPC analysis and Biomedal S.L. for supplying the pALEX2-Ca-GFP plasmid to produce C-Lyt-GFP. This work was supported by a VID1 grant from the Netherlands Organisation for Scientific Research (grant 700.56.428), the Escuela Valenciana de Estudios para la Salud (Generalidad Valenciana, Spain, Grant 95/2005) and the Fundación Salvat Inquifarma (Spain). Ciber de Enfermedades Respiratorias (CibeRes) is an initiative of Spanish Instituto de Salud Carlos III. Additional funding was provided by the COMBACT program (S-BIO-0260/2006) of the Comunidad de Madrid. V.M.H.-R. was supported by a PhD fellowship from Spanish Ministry of Education.

Supporting information for this article is available on the WWW under <http://dx.doi.org/10.1002/anie.200803664>.

ine-binding sites in C-LytA that match the multivalent arrangement of choline groups on the teichoic acid units (Figure 1). The strategy reported herein was to develop strong and highly specific inhibitors by mimicking this characteristic presentation of choline residues on the cell wall. Multivalency has been recognized as an important strategy to develop semisynthetic ligands with high affinity and specificity for biological targets.^[13] Dendrimers were chosen as attractive scaffolds that can provide well-defined multivalent ligands with enough inherent flexibility to adjust to the valency and spacing of choline-binding sites.^[14]

Choline-functionalized poly(propylene imine) dendrimers containing 4, 8, 16, or 64 choline end groups (g1-cho, g2-cho, g3-cho, and g5-cho, respectively) were readily obtained by reaction of the amine end groups of poly(propylene imine) dendrimers with activated choline (Scheme 1; Figure S1 in the Supporting Information), and they showed well-defined structures after synthesis and workup (Figure S2 in the Supporting Information). A fusion protein of C-LytA with green fluorescent protein (C-Lyt-GFP) was used to provide initial evidence for the interaction of these choline dendrimers with CBMs in solution. Addition of choline dendrimers to C-Lyt-GFP resulted in a substantial decrease in the fluorescence aniso-



Scheme 1. Chemical structures of the choline-functionalized poly(propylene imine) dendrimers used in this study.

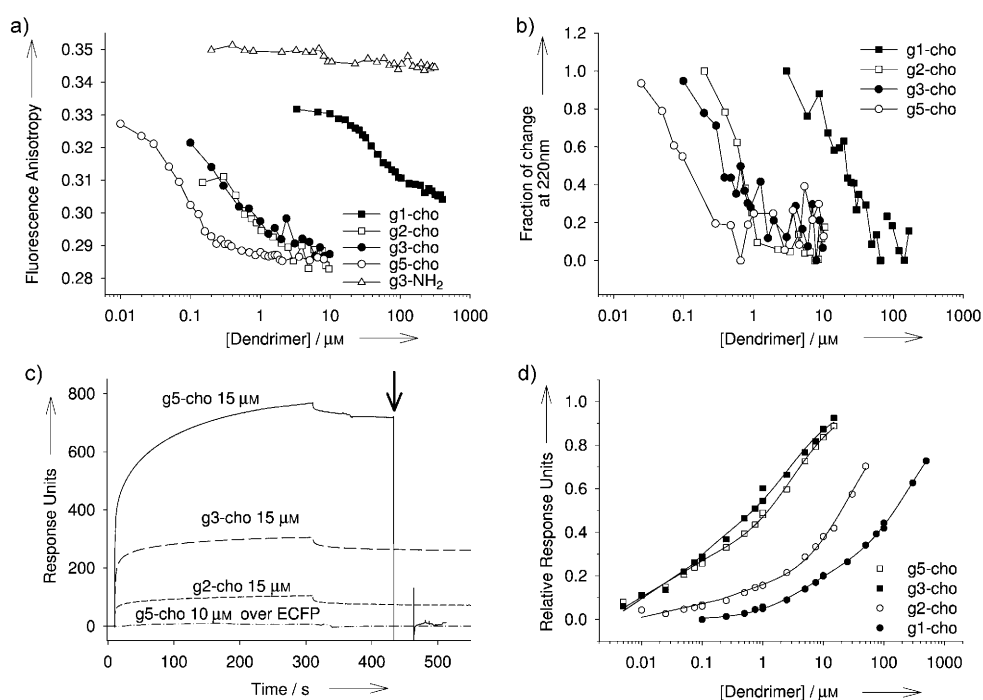


Figure 2. In vitro characterization of the interaction between choline dendrimers and CBPs. a) Binding of choline dendrimers to C-Lyt-GFP. C-Lyt-GFP (1 μM) was titrated with various generations of choline dendrimers; response was monitored by fluorescence anisotropy at 550 nm using excitation at 480 nm. b) Binding of choline dendrimers to 3 μM C-LytA monitored using CD at 220 nm. c) SPR analysis of interaction between different generations of choline dendrimers and immobilized CLyt-GFP (2000 RU). The arrow represents a 30 s injection of 1 M choline to the g5-cho experiment. The binding of 10 μM g5-cho to immobilized ECFP (2000 RU) is shown for comparison. d) Representative SPR equilibrium binding curves for choline dendrimers bound to C-Lyt-GFP obtained by the titration of a surface with 2000 RU immobilized C-Lyt-GFP with the indicated choline dendrimers. Solid lines represent the best fit of the data to a model for two binding sites (see the Supporting Information). The data were normalized according to the experimental total R_{max} (defined as the maximal response units when all sites are occupied), that was calculated as the sum of the R_{max} parameters of each binding site) obtained from the fit results, which are shown in Table S1 in the Supporting Information. All the experiments shown in this figure were performed at 20 $^{\circ}\text{C}$ in 100 mM phosphate-buffered saline at pH 7 with 500 mM NaCl. High ionic strength was used to avoid nonspecific ionic interactions of the positively charged dendrimers with the proteins.

trophy of the GFP moiety (Figure 2a), most likely as a result of energy transfer between two close GFP fluorophores assembled around a single dendrimer particle (Figure S3 in the Supporting Information). Addition of choline to C-Lyt-GFP, which promotes specific dimerization through the C-LytA module,^[5,7] also induced similar changes in anisotropy (Supporting Information Figure S3c). Importantly, the apparent affinity was strongly dependent on the dendrimer generation, showing half-maximal effects at 0.1 μM for g5-cho, 1 μM for g3-cho and g2-cho, and 100 μM for g1-cho. The change in anisotropy was specific for the interaction between choline dendrimers and C-LytA, as no changes in anisotropy were observed upon addition of a nonderivatized third-generation dendrimer (g3-NH₂) to C-Lyt-GFP (Figure 2a) or in the titration of yellow fluorescent protein alone with choline dendrimers (Figure S3b,d in the Supporting Information). At concentrations of dendrimers above 100 μM , visible aggregates appeared that could be resolubilized by the addition of free choline, suggesting that such aggregates may comprise a

network of choline dendrimers and protein cross-linked through specific multiple choline-dependent interactions.

The far-UV circular dichroism (CD) spectrum of C-LytA is dominated by the contribution of aromatic residues in the choline-binding sites.^[12] In contrast to the binding of free choline, a decrease in the CD signal was observed upon addition of choline dendrimers (Figure 2b and Figure S4 in the Supporting Information), suggesting a different conformational change in the protein. Again, the effects were observed at 0.1–1 μM concentrations for the higher-generation dendrimers, representing a 10^3 – 10^4 -fold increase of apparent affinity compared to monovalent choline.^[8,12]

Next, surface plasmon resonance (SPR) studies were performed. Specific and stable binding to immobilized C-Lyt-GFP was observed for various generations of choline dendrimers, while no binding to immobilized enhanced cyan fluorescent protein (ECFP) was detected (Figure 2c). The binding was unaffected by high salt concentrations (1M NaCl; data not shown) but was efficiently disrupted by 1M choline, which is consistent with specific binding of choline dendrimers to the C-LytA moiety. Analysis of titration experiments indicated the presence of two binding modes: a high-affinity site with dissociation equilibrium constants (K_d) of approximately 0.03 (g5-cho, g3-cho), 0.15 (g2-cho), and 4.1 μM (g1-cho); and a low-affinity site with K_d values of approximately 3 (g5-cho and g3-cho), 23 (g2-cho), and 263 μM (g1-cho; Figure 2d and Table S1 in the Supporting Information). To exclude possible effects of surface multivalency and protein immobilization, the interaction between CBMs and choline dendrimers was also studied using biotin-labeled g3-cho and g5-cho immobilized on streptavidin-functionalized SPR chips. Again, strong and specific binding was observed for CBM-containing proteins (C-LytA and C-Lyt-GFP) at low micromolar concentrations, while no relevant binding was detected for GFP (Figure S5 in the Supporting Information). The presence of two binding modes was observed, with K_d values that were similar to those obtained using immobilized C-Lyt-GFP (Table S1 and Figure S5b–e in the Supporting Information).

To test whether choline dendrimers can effectively block the binding of CBPs to the pneumococcal cell wall, their inhibitory potency was determined in vitro for the LytA amidase, LytB β -N-acetylglucosaminidase, LytC lysozyme, and Pce phosphorylcholinesterase (Table 1 and Figure S6 in the Supporting Information). These enzymes are involved in essential virulent processes, such as regulation of the availability of choline residues in the cell wall, separation of daughter cells at the end of cell division, and autolysis at the end of the stationary phase.^[15] Similar inhibitory profiles by dendrimers are observed for enzymes with totally different catalytic domains, confirming that the inhibition results from specific binding to their common CBMs. A peculiar activation of LytA and LytC is achieved at low choline concentrations, a phenomenon that has been described before,^[10] but this effect is not detected with choline dendrimers. Excellent agreement was observed between the IC_{50} values obtained for full-length LytA and the apparent affinities obtained for its isolated choline-binding module in the in vitro binding experiments, showing a 10^4 – 10^5 -fold increased potency of g2-cho, g3-cho,

and g5-cho compared to free choline (Table 1). The most pronounced increases in affinity were observed between free choline and g1-cho, and between g1-cho and g2-cho, probably reflecting an increased ability to form multiple, simultaneous interactions within the same CBM. Dendrimers beyond the second generation most likely do not improve this concurrent binding and only display a more gradual increase in affinity owing to statistical effects that favor binding of the higher-generation dendrimers.

To evaluate the effects of choline dendrimers on *S. pneumoniae* growth, we checked their effect on cell separation and autolysis in the stationary phase of a cell culture. Addition of choline dendrimers to the medium at the beginning of the exponential growth phase effectively blocked autolysis of *S. pneumoniae* R6 cultures after 17 h incubation, as deduced from the stable optical density (attenuance) values, which are directly related to the density of bacterial cells. A concentration of around 10 μM for g5-cho and g3-cho and 100 μM for g2-cho exerted a similar effect as 50 mM choline (Figure 3a and Figure S7 in the Supporting Information). At 200 μM , g1-cho did not completely block autolysis, but the attenuation after 17 h was somewhat higher than the control without additives, indicating some residual effect. Addition of 100 μM of the unfunctionalized second-generation amine dendrimer (g2-NH₂) did not induce any effect on growth, which confirms the specificity of the choline dendrimers. Microscopic analysis showed the presence of long chains of cells after 4 h of culture with 100 μM g2-cho, g3-cho, and g5-cho, but not with 100 μM g1-cho (Figure 3b). Again, a similar inhibition of cell-wall division was observed for free choline only at concentrations of 50 mM.^[9] Because no other morphological modifications were detected and cell viability remained unaffected (data not shown), these effects on growth are clearly not due to an unspecific toxicity of choline dendrimers.

Table 1: Effects of choline dendrimers on the activity of *S. pneumoniae* cell-wall-lytic enzymes.

Enzyme	IC_{50} [μM] ^[a]				
	Choline	g1-cho	g2-cho	g3-cho	g5-cho
LytA	9.1×10^3	10	0.2	0.02	0.006
LytB	6.3×10^3	4.7	5.4	3.5	0.9
LytC	2.0×10^3	60	2.2	2.9	0.3
Pce	1.9×10^3	15	0.8	0.1	0.8

[a] Concentration of choline and choline dendrimers (IC_{50}) that causes 50% inhibition of enzyme activity for the cell-wall-lytic enzymes LytA, LytB, LytC, and Pce, calculated by interpolation from the curves displayed in Figure S6 in the Supporting Information. Activity in the absence of ligands is taken as 100%.

In conclusion, choline dendrimers were developed that bind to CBMs with high affinity and specificity, yielding an attractive new class of potential antimicrobial compounds. Important advantages of these choline dendrimers over other polymer-based inhibitors of cell–protein interactions include their monodispersity and their efficacy at low valency and molecular weight. The strong complementarity between the multivalent dendritic architecture and the tandem arrange-

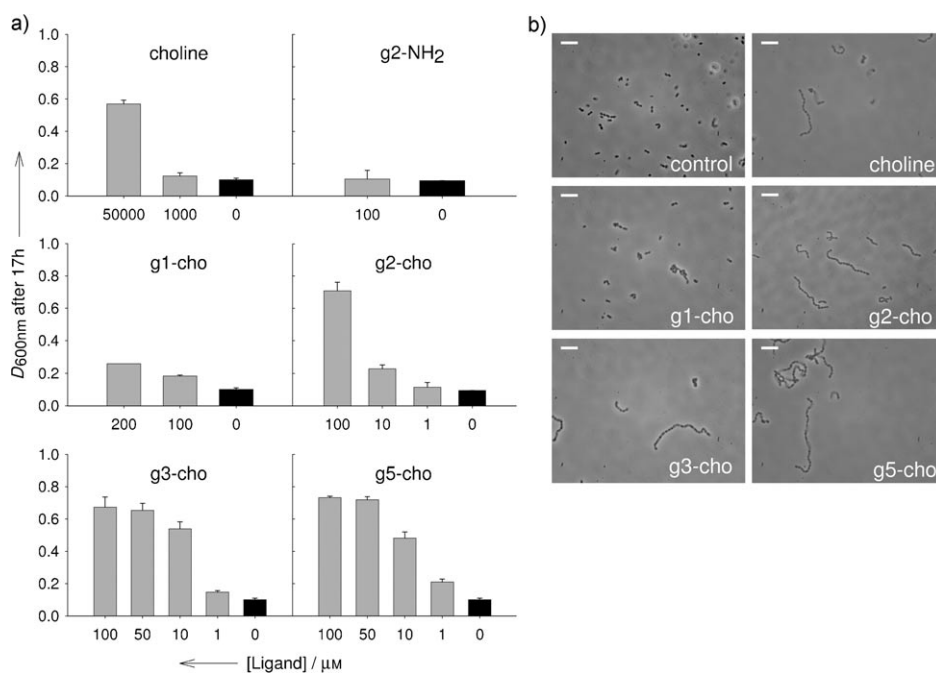


Figure 3. Effect of choline dendrimers on *S. pneumoniae* growth. a) Relative attenuation (D) of *S. pneumoniae* R6 cultures grown in the presence or absence of the indicated compounds after 17 h. Data are the average of two independent experiments. b) Phase-contrast micrographs of cultures taken after 4 h of growth in the presence or absence of 100 μM dendrimer or 50 μM choline. Bars represent 5 μm .

ment of the choline-binding repeats in pneumococcal CBMs is probably a key factor to their effectiveness as inhibitors of pneumococcal cell-wall hydrolysis.

Received: July 27, 2008

Revised: October 14, 2008

Published online: December 29, 2008

Keywords: antimicrobial agents · dendrimers · inhibitors · medicinal chemistry · multivalency

- [1] a) B. Maestro, J. M. Sanz, *Recent Patents Anti-Infect. Drug Disc.* **2007**, *2*, 188–196; b) T. Q. Tan, *Pediatr. Ann.* **2002**, *31*, 241–247.
 [2] World Health Organization, *Weekly Epidemiol. Rec.* **2007**, *82*, 93–104.
 [3] A. Tomasz, *Science* **1967**, *157*, 694–697.

- [4] S. Bergmann, S. Hammerschmidt, *Microbiology* **2006**, *152*, 295–303.
 [5] C. Fernández-Tornero, R. López, E. García, G. Giménez-Gallego, A. Romero, *Nat. Struct. Biol.* **2001**, *8*, 1020–1024.
 [6] J. A. Hermoso, B. Monterroso, A. Albert, B. Galán, O. Ahrazem, P. García, M. Martínez-Ripoll, J. L. García, M. Menéndez, *Structure* **2003**, *11*, 1239–1249.
 [7] a) J. M. Sánchez-Puelles, J. M. Sanz, J. L. García, E. García, *Gene* **1990**, *89*, 69–75; b) P. Usobiaga, F. J. Medrano, M. Gasset, J. L. García, J. L. Saiz, G. Rivas, J. Laynez, M. Menéndez, *J. Biol. Chem.* **1996**, *271*, 6832–6838.
 [8] B. Maestro, J. M. Sanz, *Biochem. J.* **2005**, *387*, 479–488.
 [9] T. Briese, R. Hakenbeck, *Eur. J. Biochem.* **1985**, *146*, 417–427.
 [10] B. Maestro, A. González, P. García, J. M. Sanz, *FEBS J.* **2007**, *274*, 364–376.
 [11] a) M. J. Jedrzejewski, *Microbiol. Mol. Biol. Rev.* **2001**, *65*, 187–207; b) D. M. Musher, R. F. Breiman, A. Tomasz in *Streptococcus pneumoniae. Molecular biology and mechanism of disease*. (Ed.: A. Tomasz), Mary Ann Liebert, Larchmont, **2000**, pp. 485–491.
 [12] F. J. Medrano, M. Gasset, C. López-Zumel, P. Usobiaga, J. L. García, M. Menéndez, *J. Biol. Chem.* **1996**, *271*, 29152–29161.
 [13] a) M. Mammen, S.-K. Choi, G. M. Whitesides, *Angew. Chem.* **1998**, *110*, 2908–2953; *Angew. Chem. Int. Ed.* **1998**, *37*, 2754–2794; b) S.-K. Choi, *Synthetic Multivalent Molecules: Concepts and Biomedical Applications*, Wiley, New York, **2004**; c) L. L. Kiessling, J. E. Gestwicki, L. E. Strong, *Angew. Chem.* **2006**, *118*, 2408–2429; *Angew. Chem. Int. Ed.* **2006**, *45*, 2348–2368.
 [14] a) A. W. Bosman, H. M. Janssen, E. W. Meijer, *Chem. Rev.* **1999**, *99*, 1665–1688; b) S. Hong, P. R. Leroueil, I. J. Majoros, B. G. Orr, J. R. Baker, Jr., M. M. Banaszak Holl, *Chem. Biol.* **2007**, *14*, 107–115; c) J. L. de Paz, C. Noti, F. Bohm, S. Werner, P. H. Seeberger, *Chem. Biol.* **2007**, *14*, 879–887.
 [15] R. López, E. García, P. García, J. L. García in *The Pneumococcus* (Eds.: E. I. Tuomanen, T. J. Mitchell, D. A. Morrison, B. G. Spratt), ASM Press, Washington, **2004**, pp. 75–88.



Supporting Information

© Wiley-VCH 2008

69451 Weinheim, Germany

Supporting Information

Multivalent Choline Dendrimers as Potent Inhibitors of Pneumococcal Cell Wall Hydrolysis

Víctor M. Hernández-Rocamora¹, Beatriz Maestro¹, Bas de Waal², María Morales³, Pedro García³, E.W. Meijer², Maarten Merkx^{2,*}, Jesús M. Sanz^{1,*}

¹Instituto de Biología Molecular y Celular, Universidad Miguel Hernández, Av. Universidad, s/n, E-03202 Elche (Alicante), Spain. ²Laboratory of Chemical Biology, Department of Biomedical Engineering, Eindhoven University of Technology, 5600 MB Eindhoven, The Netherlands. ³Departamento de Microbiología Molecular, Centro de Investigaciones Biológicas (CSIC) and Ciber de Enfermedades Respiratorias (CibeRes), Ramiro de Maeztu, 9, 28040 Madrid, Spain.

* Correspondence should be addressed to J.M.S. (jmsanz@umh.es) or M.M. (m.merkx@tue.nl)

Methods	7
Figure S1	14
Figure S2	15
Figure S3	16
Figure S4	17
Figure S5	18
Figure S6	19
Figure S7	20
Table S1	21
References	22

Methods

Dendrimer synthesis

General

Solvents were obtained from Biosolve and were of p.a. quality. Di (N-succinimidyl) carbonate (Fluka), dialysis tubing (Spectrum Labs), and choline chloride (> 99%, Fluka) were used as received. Poly(propylene imine) dendrimers were obtained from SyMO-Chem BV (Eindhoven, The Netherlands). Acetonitrile was stored on 4 Å activated molecular sieves (Merck) under an argon gas atmosphere. Triethylamine (>99%, Fluka) was stored on potassium hydroxide pellets (Merck). Ion exchange resin DOWEX 1X8-50 (Cl⁻ form) was obtained from Acros. Prior to use, a column was first washed with demineralised water, followed by washing with methanol. A methanolic solution of the dendrimer was applied to the column and eluted with methanol. Weakly basic ion exchange resin Amberlite IRA-95 (Aldrich) was washed with water, methanol, and again water before use. PD-10 columns (GE Healthcare) were washed with water according to the manual. Reactions were performed under a dry argon gas atmosphere.

[2-(2,5-Dioxo-pyrrolidin-1-yloxy)carbonyloxy]-ethyl]-trimethyl-ammonium; chloride (“choline NHS carbonate”)

Choline chloride (1.55 g; 11.10 mmol) was vigorously magnetically stirred with acetonitrile (30 mL) and triethylamine (1.9 mL; 13.9 mmol). Di (N-succinimidyl) carbonate (5.70 g; 22.25 mmol; 2 eq) was added and stirring was continued for 2 h. The mixture was filtered over a glass filter in a nitrogen gas atmosphere. It was washed three times with 10 mL acetonitrile. Then the product was dried at 30-40 °C *in vacuo* over P₂O₅ for an hour. It was stored in a desiccator over P₂O₅.

Yield: 1.66 g (5.91 mmol; 53% based on choline chloride) of a white very hygroscopic powder. According to ¹H NMR the product was 95% pure and it was used without further purification. ¹H NMR (DMSO-D₆, 200 MHz) δ 4.90-4.75 (m, 2H), 3.90-3.80 (m, 2H), 3.15 (s, 9H), 2.80 (s, 4H) ppm. ¹³C NMR (DMSO-D₆, 50 MHz) δ 170, 151.0, 65.2, 63.6, 53.2, 25.8 ppm. FTIR neat cm⁻¹ 1816 (s), 1784 (m), 1739 (vs), 1491 (w), 1230 (vs), 1201 (vs).

1st generation choline dendrimer (g1-cho)

DAB-*dendr*-(NH₂)₄ (100 mg; 0.316 mmol) was dissolved in 10 mL of 4/1 THF/water and 200 μL of triethylamine. Then choline NHS carbonate (380 mg) was portion wise added during 1 min. After stirring for 16 h at room temperature, the reaction mixture was evaporated. The methanolic solution of the dendrimer was applied to an IRA-95 column and eluted with methanol. Then a methanolic solution was applied to a DOWEX 1X8-50 column and eluted with methanol. This was followed by dialysis (molecular weight cut off = 500 D) versus water containing 1% of triethylamine, followed by water. After lyophilization, 111 mg product was obtained as a white powder (yield = 35.8% based on dendrimer).

¹H NMR (D₂O, 200 MHz): δ 4.45-4.30 (m, 8H, OCH₂), 3.3.6-3.5 (m, 8H, OCH₂CH₂), 3.05 (s, 36H, CH₃), 3.0 (t, 6H, CH₂NHC(O)), 2.4-2.3 (m, 12H, CH₂N), 1.60-1.45 (m, 8H, NCH₂CH₂CH₂N), 1.35-1.25 (m, 4H, NCH₂CH₂CH₂CH₂N) ppm.

¹³C NMR (D₂O, 50 MHz): δ 157.0; 64.9; 58.4; 53.6; 52.8; 50.2; 38.7; 25.3; 23.3. FTIR neat: cm⁻¹ 3553 (w), 3223 (w), 2944 (w), 1706 (vs), 1538 (s), 1479 (s), 1248 (vs).

EI-MS: Calc. C₄₀H₈₈N₁₀O₈⁴⁺: m/z 209.16; Found: m/z 209.2;

2nd generation choline dendrimer (g2-cho)

DAB-*dendr*-(NH₂)₈ (214 mg; 0.276 mmol) was dissolved in 10 mL of 4/1 THF/water, and 600 μL (4.42 mmol) of triethylamine. Choline NHS-carbonate (819 mg; 2.76 mmol) was portion wise added during 1 min, resulting in a clear solution. After 4 h of stirring at room temperature, the mixture was concentrated on a rotary evaporator. The product was dissolved in 6 mL of water and filtered over a small piece of glass wool to remove small amounts of precipitate. To this was added 2.5 mL of triethylamine, and the mixture was fractionated with water on a PD-10 column. Fractions containing choline chloride were concentrated and reapplied to the column in order to maximize the yield. This was followed by treatment of a methanolic solution of the dendrimer on a DOWEX 1X8-50 column. Yield: 400 mg (80% based on dendrimer) of a white powder.

¹H NMR (D₂O, 200 MHz): δ 4.45-4.30 (m, 16H), 3.60-3.50 (m, 16H), 3.10 (s, 72H), 3.0 (t, 16H), 2.40-2.20 (m, 36H), 1.60-1.40 (m, 24H), 1.40-1.25 (m, 4H) ppm.

¹³C NMR (D₂O, 100 MHz): δ 156.9; 64.8; 58.4; 53.7; 52.7, 51.3; 50.8; 50.2; 38.9; 25.4; 23.44; 21.9 ppm.

FTIR neat: cm⁻¹ 3355 (w), 3221 (w), 2944 (w), 1706 (vs), 1537 (s), 1478 (s), 1248 (vs). DIP EI-MS: Calc. C₈₈H₁₉₂N₂₂O₁₆⁸⁺: m/z 226.6; Found: m/z 226.8.

3rd generation choline dendrimer (g3-cho)

DAB-*dendr*-(NH₂)₁₆ (64 mg; 0.038 mmol) was dissolved in 5 mL 4/1 THF/water and 180 μL of triethylamine was added. Then choline NHS carbonate (207 mg; 0.74 mmol) was portion wise added to the vigorously stirred solution during 1 min. After stirring for 18 h at room temperature, the solution was concentrated on a rotary evaporator. It was first passed over an IRA-95 column (methanol), followed by a DOWEX 1X8-50 column (methanol). After fractionation of an aqueous solution with a PD-10 column, and lyophilization, 95 mg of product was obtained as a white powder (yield = 57.8% based on dendrimer). ¹H NMR (D₂O, 400 MHz): δ 4.45-4.35 (m, 32 H), 3.65-3.55 (m, 32H), 3.2 (s, 144H), 3.0 (t, 36H), 2.45-2.30 (m, 84H), 1.60-1.45 (m, 56H), 1.35-1.30 (m, 4H). ¹³C NMR (D₂O, 100 MHz): δ 156.9, 64.9, 58.4, 53.7, 51.3, 50.8, 50.3, 38.9, 25.7, 25.4, 21.9. FTIR neat: cm⁻¹ 3359 (w), 3229 (w), 2945 (w), 1706 (vs), 1537 (s), 1478 (s), 1248 (vs).

5th generation choline dendrimer (g5-cho)

DAB-*dendr*-(NH₂)₆₄ (80 mg; 0.01 mmol) was dissolved in 5 mL of 4/1 THF/water, and 200 μL of triethylamine (1.46 mmol). Choline NHS carbonate (240 mg; 0.857 mmol) was added portion wise during 1 min, resulting in a clear solution. After stirring for 19 h at room temperature, the reaction mixture was evaporated. A methanolic solution was passed over an IRA-95 column. The product was redissolved in methanol and passed over a DOWEX 1X8-50 column. The product was redissolved in water and some triethylamine, and fractionated over a PD-10 column. After lyophilization, 100 mg of dendrimer was obtained as a white powder (yield = 51% based on dendrimer). ¹H NMR (D₂O, 400 MHz): δ 4.50-4.35 (m, 128H), 3.70-3.55 (m, 128H), 3.10 (s, 576H), 3.0 (broad t, 128H), 2.50-2.30 (m, 372H), 1.60-1.45 (m, 246H) ppm. ¹³C NMR (D₂O, 100 MHz): δ 156.9, 64.9, 58.5, 53.8, 51.5, 50.8, 50.3, 39.0, 25.5, 22.0. FTIR neat: cm⁻¹ 3357 (w), 3229 (w), 2946 (w), 1706 (vs), 1538 (s), 1478 (s), 1248 (vs).

3rd generation choline dendrimer with approximately 1 biotin per dendrimer.

N-(13-Amino-4,7,10-trioxatridecanyl) biotinamide¹ (24 mg; 0.053 mmol) was dissolved in 1 mL of dichloromethane and was injected with a syringe into a solution of di-*tert*-butyl tricarbonate (16.0 mg, 0.061 mmol) in 1 mL of dichloromethane. The reaction was monitored by FTIR (isocyanate peak at 2277

cm⁻¹) and after 35 min, the solution was dropwise added during 3 min to a vigorous stirred solution of DAB-*dendr*-(NH₂)₁₆ (78 mg; 0.0462 mmol) in 2 mL of dichloromethane.

After 10 min, FTIR indicated disappearance of the isocyanate peak and the solution was evaporated. The oil was dissolved in 5 mL of 4/1 THF/water and 200 µL of triethylamine was added. Then choline NHS carbonate (244 mg; 0.869 mmol) was added in one portion and the clear solution was stirred for 18 h at room temperature. After dialysis versus water (molecular weight cut off = 2 kDa) and lyophilization, the product was obtained as a white powder. ¹H NMR (CD₃OD, 200 MHz): δ 4.60-4.45 (m), 3.80-3.60 (m), 3.27-3.23 (m), 3.20-3.15 (t), 2.60-2.40 (m), 1.80-1.50 (m), 1.35 (4H) ppm.

5th generation choline dendrimer with approximately 2 biotins per dendrimer.

A solution of N-(13-Amino-4,7,10-trioxatridecanyl) biotinamide¹ (19 mg, 0.042 mmol) in 1 mL of dichloromethane was injected into a well-stirred solution of di-*tert*-butyl tricarbonate (11 mg, 0.042 mmol) in 1 mL of dichloromethane. After 5 min of stirring, FTIR showed completion of reaction and the solution was dropwise added during 2 min to a solution of DAB-*dendr*-(NH₂)₆₄ (157 mg; 0.02093 mmol) in 5 mL of dichloromethane. After 3 h of stirring at room temperature, the solution was concentrated on a rotary evaporator to yield an oil weighing 149 mg.

50 mg of this oil (6.05 mmol dendrimer) was dissolved in 4 mL of a 1/1 THF/water mixture and triethylamine was added (400 µL). Choline NHS carbonate (105 mg, 0.374 mmol) was added, followed by another amount of choline NHS carbonate (112 mg, 0.399 mmol) 20 min later. The clear reaction solution was stirred for an additional 3.5 h and was then dialyzed (molecular weight cut off = 1 kDa) first versus water containing 1% of triethylamine, followed by dialysis versus water. After lyophilization the yield was 84 mg of a white powder.

¹H NMR (CD₃OD, 200 MHz): δ 4.60-4.40 (m), 3.80-3.60 (m), 3.27-3.25 (m), 3.20-3.10 (t), 2.60-2.30 (m), 1.85-1.50 (m) ppm.

Expression and purification of C-LytA and C-Lyt-GFP

C-LytA was purified by affinity chromatography from the overproducing *Escherichia coli* strain RB791 [pCE17] as previously described². The eluted protein was extensively dialyzed against 10 mM NH₄HCO₃ at pH 7 and freeze-dried for 24 h at -80 °C.

C-Lyt-GFP expression was achieved from the REG1 [pALEX2-Ca-GFP] strain generously donated by Biomedal, S.L. C-Lyt-GFP is a fusion protein composed of the C-LytA domain in the N-terminal and GFP[LVA]³, a GFPmut3.1 derivative, in the C-terminal, connected via a 28 amino acid linker. Expression was carried out using the C-LYTAG Purification System (Biomedal, S.L.) as described by the manufacturer.

Surface Plasmon Resonance

Measurements were performed on a Biacore T100. Buffers were prepared fresh and 0.22 µm-filtered before use. Covalent immobilization of C-Lyt-GFP on a commercial Biacore CM5 chip was performed using the Amine Coupling kit (Biacore Inc., BR-1000-50) according to manufacturer's instructions. For control experiments in which ECFP S208F was immobilized instead of C-Lyt-GFP, the same coupling conditions were used. In all the experiments, samples were flown first through a reference flow cell with no molecules immobilized. In experiments with proteins immobilized, the reference channel carboxyl groups were blocked with amine groups by performing a standard amine coupling reaction but flowing only 1 M ethanolamine after surface activation. In experiments with dendrimers immobilized, 10 mM NaOH+1 M NaCl was used to eliminate remaining bound protein at the end of each cycle, while in experiments with protein immobilized, 1 M choline was used to remove remaining bound dendrimers. Protein and dendrimer titrations were both done in 100 mM PBS at pH 7 with 50 mM or 500 mM NaCl, injecting buffer three times before beginning the titration and injecting at least one of the concentrations in duplicate. Binding curves were obtained from titrations by plotting the response level at equilibrium (flat response level after injection) against the protein concentration injected.

Analysis of Surface Plasmon Resonance data

Binding curves were fitted using the non-linear least squares method to a model for two different binding sites described by equation 1:

$$(1) \quad R = \frac{R_{MAX1} \cdot C}{K_{D1} + C} + \frac{R_{MAX2} \cdot C}{K_{D2} + C}$$

where R is the Biacore signal when the binding arrives at the equilibrium, R_{MAX1} and R_{MAX2} are the maximum responses for site 1 and site 2 respectively, K_{D1} and K_{D2} are dissociation constants for site 1 and site 2 respectively, and C is the analyte concentration.

Analyte:ligand ratios in Table 1 were calculated as follows. The experimental total R_{MAX} (the sum of $R_{MAX1} + R_{MAX2}$) indicates the maximum amount of analyte that the surface can capture. Theoretical total R_{MAX} which is the maximum binding signal expected for any amount of immobilized molecules can be calculated with the formula (BIAcore Instruction Manual):

$$(2) \quad R_{MAX} = \frac{analyteMW}{ligandMW} \cdot S_M \cdot R_L$$

where $ligandMW$ and $analyteMW$ are the molecular weights of the immobilized molecule and the molecule that binds to it, respectively; R_L is the amount of molecule immobilized in RUs and S_M is the ratio of free molecules bound per immobilized molecule bound. Substituting the experimental total R_{MAX} in (2) one can calculate the apparent S_M value, which is an indication of the amount of analyte molecules that are captured per immobilized ligand molecules.

Fluorescence

Samples measured contained protein at the specified concentrations dissolved in 100 mM PBS at pH 7 with 500 mM NaCl. Measurements were performed on a Varian Cary Eclipse fluorescence spectrophotometer using a 1 cm light path cuvette. Emission scans were recorded using an excitation wavelength of 480 nm and emission was collected from 500 to 600 nm. Fluorescence anisotropy measurements were registered using an excitation wavelength of 480 nm and emission was collected either from 545 to 555 nm or from 530 to 540 nm. The anisotropy values from each wavelength were averaged. Standard deviation of this average is displayed in titration curves.

Circular dichroism

Circular dichroism (CD) experiments were performed in a Jasco J-810 spectropolarimeter equipped with a Peltier PTC-423S system. Isothermal wavelength spectra were acquired at a scan speed of 50 nm/min with a response time of 2 sec and averaged over at least four scans at 20 °C. Protein concentration was 3 μ M unless otherwise stated, and the cuvette path length was 0.1 cm.

Bacterial strains and growth conditions

S. pneumoniae R6 is a derivative of the Rockefeller University strain R36A. The *E. coli* strains harboring recombinant plasmids encoding the different proteins used in this work were as follows: RB791

[pCE17] for C-LytA², BL21 (DE3) [pRGR5] for LytB⁴, RB791 [pGL100] for LytA⁵, BL21 (DE3) [pLCC14] for LytC⁶, and BL21 (DE3) [pRGR12] for Pce⁷. Pneumococcal cultures were grown without aeration in C medium supplemented with 0.08% (w/v) yeast extract (C + Y medium)⁸. Growth was monitored by measuring the attenuation (D) in a Thermo Spectronic spectrophotometer (Waltham, MA, USA). *E. coli* cultures were grown with aeration in LB medium with ampicillin (100 mg ml⁻¹).

In vitro assays of pneumococcal cell wall lytic enzymes

Extracts of *E. coli* overexpressing the LytA, LytB, LytC and Pce enzymes were used for cell wall degradation assays, performed basically as previously described⁹, using pneumococcal cell walls labeled with [*methyl*-³H] choline (500 cpm. μL^{-1} , approximately 0.7 $\mu\text{g } \mu\text{L}^{-1}$) as substrate, and measuring the amount of radioactivity released into the supernatant, corresponding to solubilized fragments of the cell wall. Experimental conditions depended on the enzyme, and were set as follows: 37 °C and pH 6.9 for LytA and LytB; 30 °C and pH 6.0 for LytC; and 30 °C and pH 6.9 for Pce.

Figure S1

Scheme of the derivatization of polypropyleneimine dendrimers with choline.

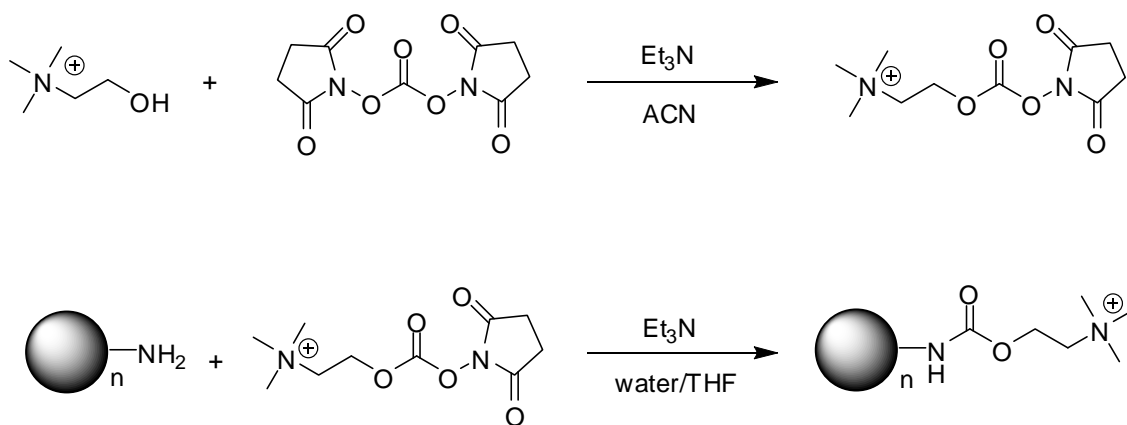


Figure S2

Characterization of choline dendrimers using Gel Permeation Chromatography (GPC). GPC was performed on a TSK-G 4000 PWx column (300×7.5 mm) in a buffer of 0.1 M citric acid and 0.025% sodium azide. The flow rate was set at 0.5 mL/min and refractive index (RI) was used for detection. The small shoulders present at the peaks of **g5-cho** and **g3-cho** probably represent the presence of some dendrimer dimer. The poly(propyleneimine) dendrimers that were used as starting compounds also contained small amounts of dimers.

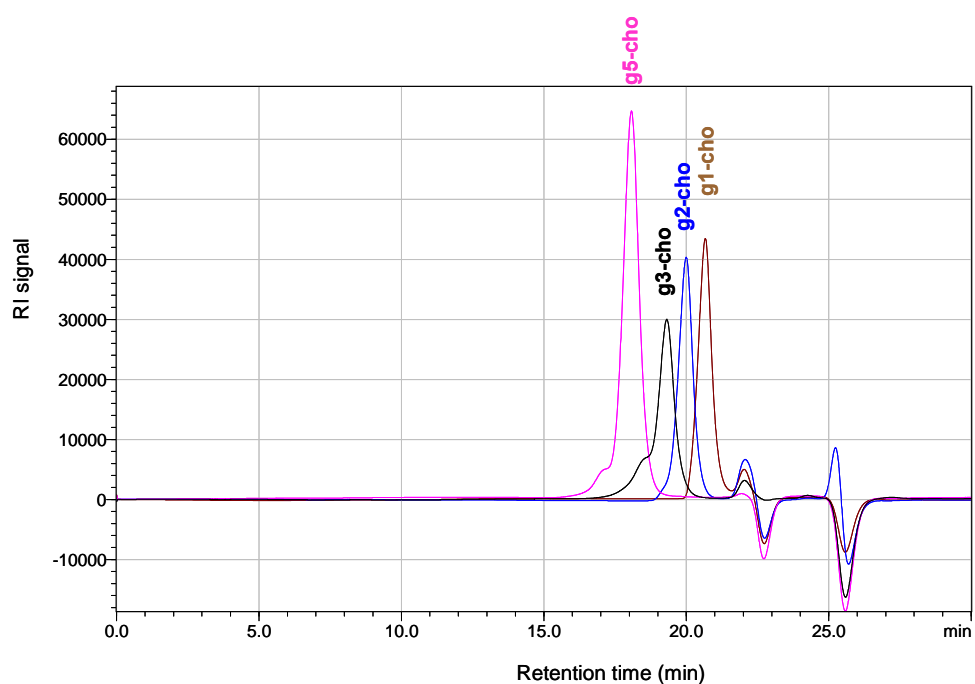


Figure S3

Additional fluorescence data. **(a)** Fluorescence spectra of C-Lyt-GFP in the absence of choline: excitation spectrum monitoring emission at 550 nm (black line), and emission spectrum upon excitation at 450 nm (red line). **(b)** Fluorescence spectra of hexahistidine-tagged yellow fluorescent protein (His₆-YFP) in the absence of choline: excitation spectrum monitoring emission at 570 nm (black line), and emission spectrum upon excitation at 470 nm (red line). **(c)** Titration of 1 μ M C-Lyt-GFP with choline, followed by fluorescence anisotropy, exciting at 500 nm and measuring emission anisotropy at 460-470nm. **(d)** Titration of 1 μ M His₆-YFP with **g3-cho**. Same conditions as in **(c)**. Spectra in **(a)** , **(b)** and **(c)** were taken in 100 mM PBS at pH 7 with 50 mM NaCl. In **(d)** the same buffer but with 500 mM NaCl was used.

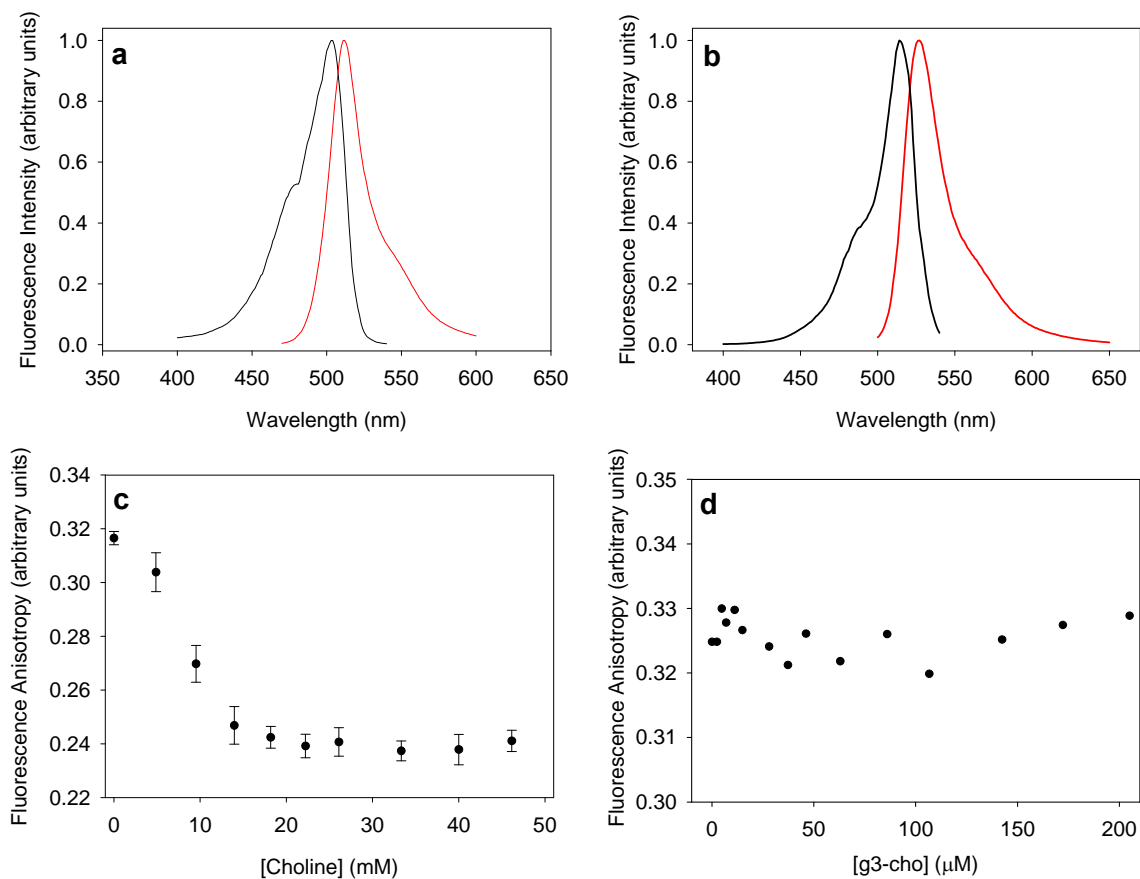


Figure S4

Changes in the far-UV circular dichroism spectrum of C-LytA caused by choline or by choline dendrimers. Spectra were taken in 100 mM PBS at pH 7 with 50 mM NaCl at 20 °C. Protein concentration was 3 μ M.

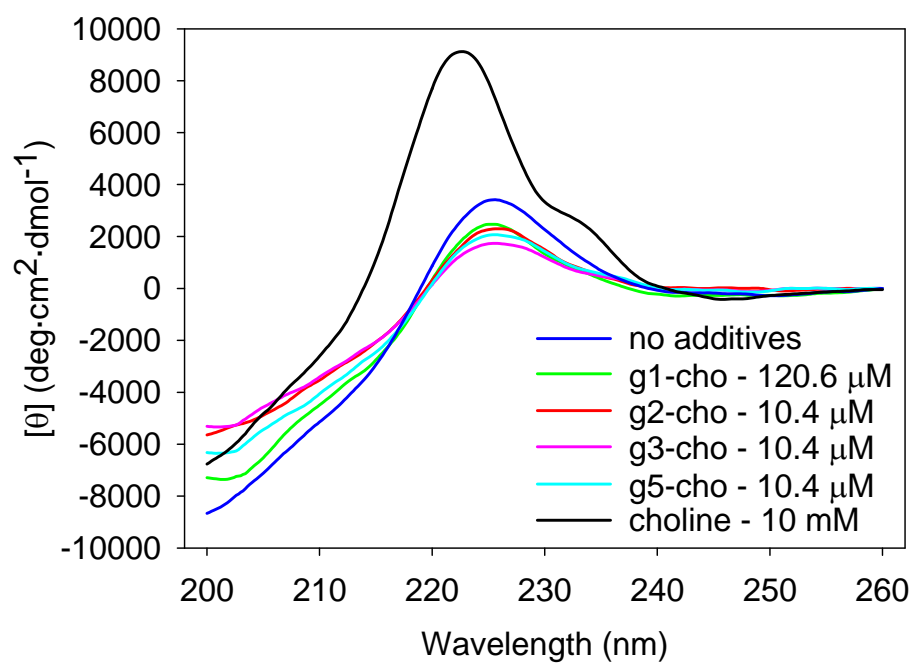


Figure S5

C-LytA and C-Lyt-GFP binding to immobilized biotin-labeled choline dendrimers studied by SPR. **(a)** C-LytA, C-Lyt-GFP and GFP sensorgrams at a surface with 500 RU of immobilized biotin-labeled g5-cho. **(b-e)** Representative SPR equilibrium binding curves obtained by titrating a surface with 500 RU immobilized biotin-labeled choline dendrimers with either C-LytA or C-Lyt-GFP. “Analyte” is the molecule being titrated and “ligand” the molecule attached to the surface. Solid lines represent the best fit of the data to a model for two binding sites (Methods, eq. 1). The K_D values obtained from these fits are listed in **Table S1**. All SPR experiments were performed at 20 °C using 100 mM PBS at pH 7 with 500 mM NaCl.

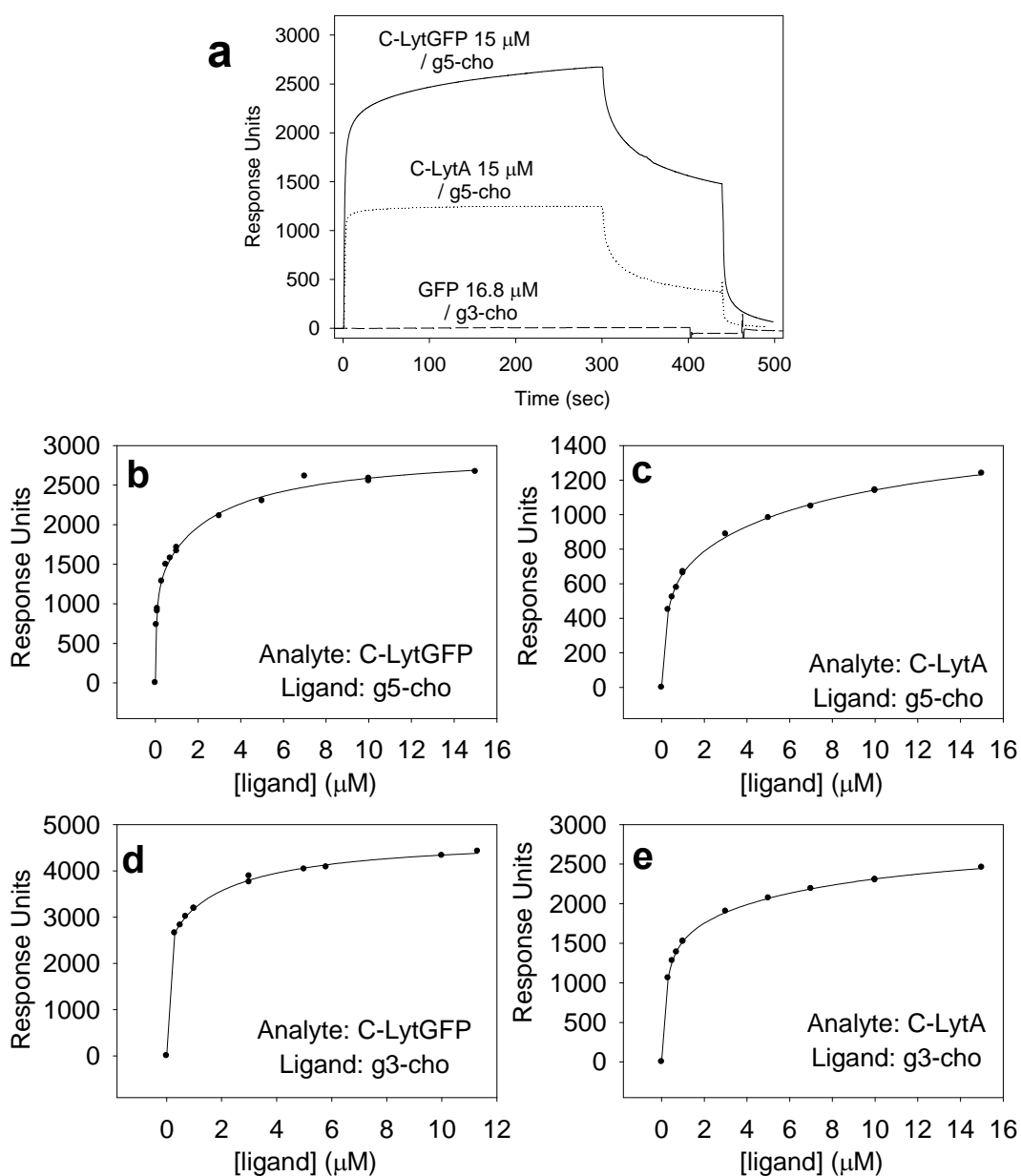


Figure S6

Effect of choline dendrimers on the activity of *S. pneumoniae* cell wall lytic enzymes. Four *S. pneumoniae* cell wall lytic enzymes, LytA, LytB, LytC and Pce, were assayed as described in **Methods**, in the presence or absence of choline or choline dendrimers. Data are shown as the percentage of activity with respect to the enzyme in the absence of any ligands, and are the average of three independent experiments. A dashed line has been included to show the level of 100 % activity.

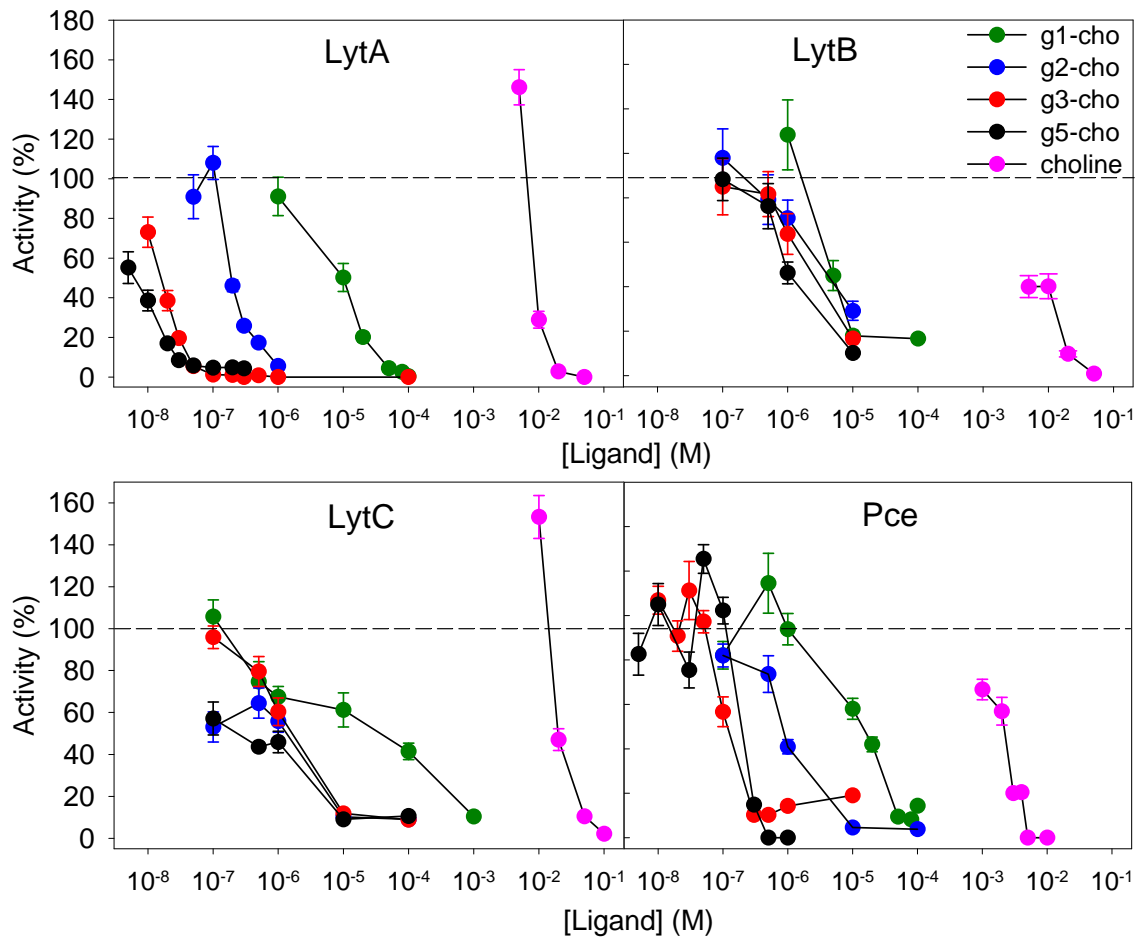


Figure S7

Effect of choline dendrimers on *S. pneumoniae* R6 growth. The growth of *S. pneumoniae* R6 liquid cultures in the presence or absence of choline, choline dendrimers or polypropyleneimine dendrimers was measured by monitoring attenuation of the cultures over 17 h.

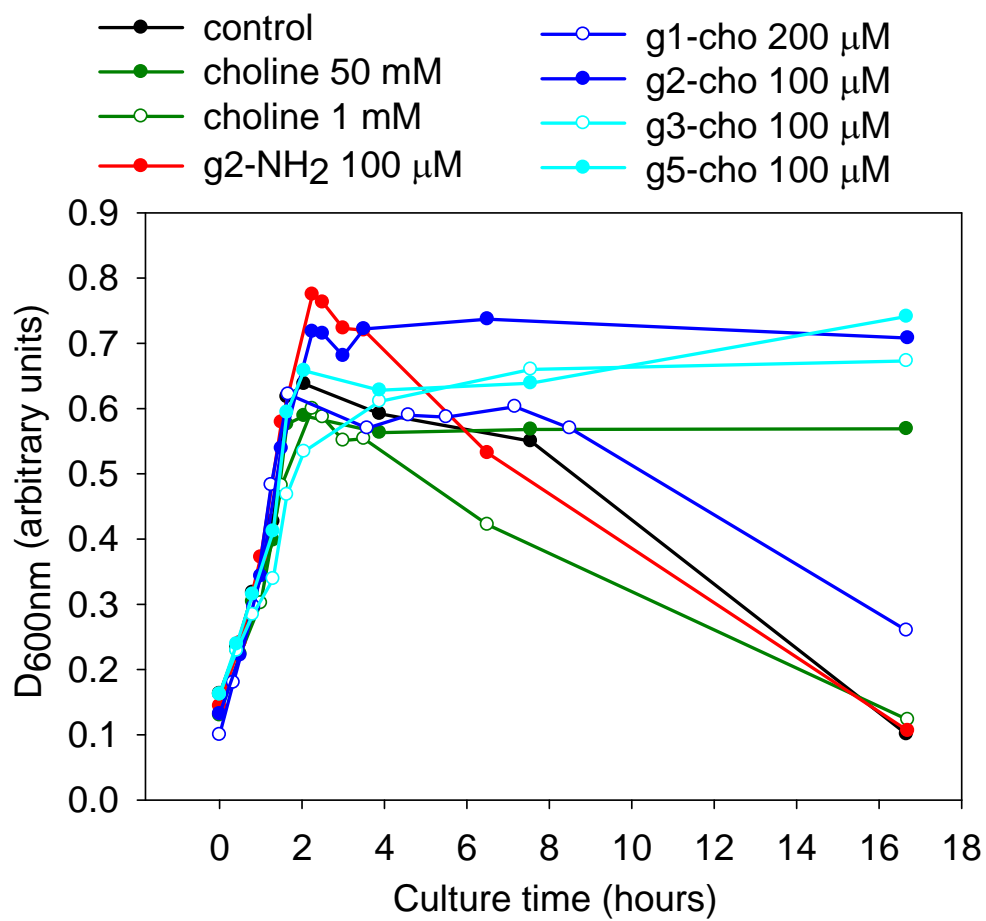


Table S1

Binding affinities obtained in SPR experiments with different proteins and dendrimer generations.

Analyte	Ligand	Kd₁ (μM)	Kd₂ (μM)	analyte : ligand
g1-cho	C-Lyt-GFP	4.1 ± 1.0	263 ± 52	2.3
g2-cho	C-Lyt-GFP	0.15 ± 0.05	23 ± 5	2.3
g3-cho	C-Lyt-GFP	0.05 ± 0.01	2.5 ± 0.8	1.7
g5-cho	C-Lyt-GFP	0.023 ± 0.004	3.0 ± 0.4	1.1
C-LytA	g3-cho	0.19 ± 0.01	8.3 ± 1.2	1.6
C-LytA	g5-cho	0.21 ± 0.04	8.4 ± 2.4	3.5
C-Lyt-GFP	g3-cho	0.02 ± 0.02	2.2 ± 0.6	0.8
C-Lyt-GFP	g5-cho	0.05 ± 0.01	2.8 ± 0.8	2.0

References

1. Charvet, N., Reiss, P., Roget, A., Dupuis, A., Grünwald, D., Carayon, S., Chandezon F. & Livache, T. *J. Mater. Chem.* **14**, 2638-2642 (2004).
2. Sánchez-Puelles, J.M., Sanz, J.M., García, J. L. & García, E. *Gene* **89**, 69-75 (1990).
3. Andersen, J. B. *et al. Appl. Environ. Microbiol.* **64**, 2240-2246 (1998).
4. de las Rivas, B., García, J.L., López, R. & García, P. *J. Bacteriol.* **184**, 4988-5000 (2002).
5. García, J.L., García, E. & López, R. **149**, 52-56 (1987).
6. García, P., González, M.P., García, E., García J.L., & López, R. *Mol. Microbiol.* **33**, 128-138 (1999).
7. de las Rivas, B., García, J.L., López, R. & García, P. *Microb. Drug Resist.* **7**, 213-222 (2001).
8. Lacks, S. & Hotchkiss, R.D. *Biochim. Biophys. Acta* **39**, 508-517 (1960).
9. Mosser, J.L. & Tomasz, A. *J. Biol. Chem.* **245**, 287-298 (1970).